Journal of Alloys and Compounds 509 (2011) 2496–2502

Contents lists available at ScienceDirect

Journal of Alloys and Compounds

journal homepage: www.elsevier.com/locate/jallcom

The dielectric and electric properties of $(Ba_{0.68-x}Sr_{0.311}Bi_{0.006}Mg_x)(Ti_{0.99}Sn_{0.01})O_3$ ceramics

Shiguo Xu*, Yuanfang Qu*, Dean Yang

Key Laboratory for Advanced Ceramics and Machining Technology of Ministry of Education, College of Materials Science & Engineering, Tianjin University, Tianjin 300072, China

ARTICLE INFO

Article history:
Received 25 August 2010
Received in revised form 4 November 2010
Accepted 10 November 2010
Available online 17 November 2010

Keywords:
Ceramics
Dielectric properties
Electric conduction
Phase transitions
Grain size

ABSTRACT

$(Ba_{0.68-x}Sr_{0.311}Bi_{0.006}Mg_x)(Ti_{0.99}Sn_{0.01})O_3$ ceramics were prepared by conventional solid state reaction method. The influences of Mg^{2+} content on structure, dielectric and electric properties of the sintered specimens were investigated. At lower Mg^{2+} concentrations ($x \leq 0.015$), Mg^{2+} replaced Bi^{3+} at the A-site in the perovskite structure, which made dielectric constant to obey the Curie–Weiss law above the phase transition temperature. The Bi^{3+} expelled from the lattice by Mg^{2+} were concentrated at grain surfaces, which caused significant decrease in grain size and ε_{max}. At higher Mg^{2+} concentrations ($x > 0.015$), Mg^{2+} acted as an acceptor dopant to replace Ti^{4+} at the B-site of the perovskite structure, leading to a deformation of the cubic lattice and making dielectric behavior to deviate from the Curie–Weiss law above the phase transition temperature. In high temperature region, the conduction carriers of all samples were controlled by $V_O^{\cdot\cdot}$.

1. Introduction

Dielectric and ferroelectric materials have been widely employed in various industrial applications, such as dynamic random access memory, microwave filters, voltage controlled oscillators and telecommunication technologies [1–4]. Conventional dielectric and ferroelectric are mainly lead-based ceramic material, which has been considered to be a serious threat to the environment [5]. Therefore, there has been a strong demand to develop lead-free ceramics, whose dielectric properties should be comparable to those of their lead-containing counterparts. Many attentions have been paid to improve the dielectric properties of $BaTiO_3$ ceramic via partial substitution of either Ba-ions (A-site doping) or Ti-ions (B-site doping) [6]. So far, many new solid solutions with excellent properties have been developed, such as $Ba_{1-x}Sr_xTiO_3$ [7], $BaTi_{1-x}Sn_xO_3$ [8–10] and $(BaSr)(SnTi)O_3$ [11,12] ceramics. Among them, stannum-containing titanate ceramics (TS) exhibited promising dielectric properties [8–19]. Aldica et al. [9] prepared dense $Ba(Ti_{1-x}Sn_x)O_3$ ($x = 0.13$) ceramic by spark plasma sintering and suggested that the influence of degree of compositional disorder on the average transition temperature can be attributed to the disorder-related variation of the average diameter of the oxygen octahedral surrounding ferroelectric ions in the perovskite structure. Du et al. [18] have studied dielectric properties and phase transition of $Ba(Sn_xTi_{1-x})O_3$ solid solution and observed diffuse phase transitions at $x \geq 0.10$. Liu et al.'s [19] study indicated that relaxor ferroelectric behavior of $Ba(Sn_xTi_{1-x})O_3$ ceramics at high x was rather associated with the suppression of homogeneous strain distortion below T_m induced by the inhomogeneous distribution of the dopant Sn ions leading in turn to the suppression of transverse correlation of the pre-existing $1-d$ polar nano-regions (below T_m). As known to all, when Mg is substituted for A site in $BaTiO_3$-based ferroelectric ceramics, the Curie peak of materials may be pressed and broadened. In addition, dielectric relaxor behavior was observed in Bi-doped $(Ba_{1-x}A_x)(Ti_{1-y}B_y)O_3$ (A=Sr or B=Zr) lead-free perovskite-type ceramics systems [20,21].

In this paper, the influences of Mg^{2+} content on structure, dielectric and electric properties of $(Ba_{0.68-x}Sr_{0.311}Bi_{0.006}Mg_x)(Ti_{0.99}Sn_{0.01})O_3$ ceramics prepared by conventional solid state reaction method were studied. Furthermore, underlying mechanisms of the effect were also discussed.

2. Experimental

Polycrystalline ceramic samples with a composition of $(Ba_{0.68-x}Sr_{0.311}Bi_{0.006}Mg_x)(Ti_{0.99}Sn_{0.01})O_3$ (B6M, $x = 0.000$, 0.005, 0.010, 0.015, 0.020, 0.025 and 0.030, abbreviated as B6M0, B6M5, B6M10, B6M15, B6M20, B6M25 and B6M30, respectively) were prepared by solid-state reaction. Raw materials used were high purity TiO_2 (>98.0%), $BaCO_3$ (>99.0%), $SrCO_3$ (>99.0%), SnO_2 (>99.0%), Bi_2O_3 (>98.0%) and $(MgCO_3)_4{\cdot}Mg(OH)_2{\cdot}5H_2O$ (>99.0%). They were mixed by ball-milling. The mixtures were dried and then calcined at 1080 °C for 2 h. All calcined powders were mixed with 0.2 at.% ZnO and 0.2 at.% MnO_2, reground, dried, granulated (with polyvinyl alcohol as a binder for granulation), pressed into pellet ($\Phi \times d = 15.00\,mm \times 2.00\,mm$) at 170 MPa. They were sintered at 1280–1340 °C for 2 h in the air. Silver paste was coated on both sides as electrodes for dielectric measurements. The coated samples were fired at 850 °C for 20 min.

* Corresponding author. Tel.: +86 22 27401940; fax: +86 22 27401940.
E-mail addresses: xushg@tju.edu.cn (S. Xu), yfqu@tju.edu.cn (Y. Qu).

0925-8388/$ – see front matter © 2010 Elsevier B.V. All rights reserved.
doi:10.1016/j.jallcom.2010.11.064

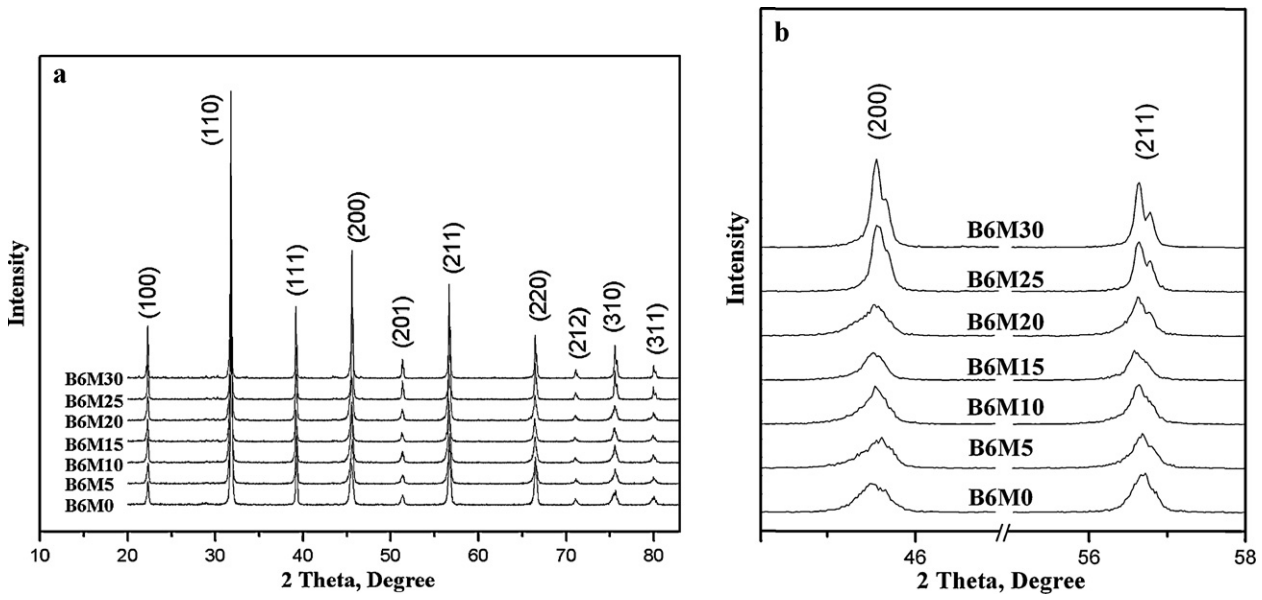

Fig. 1. XRD patterns of all sintered samples.

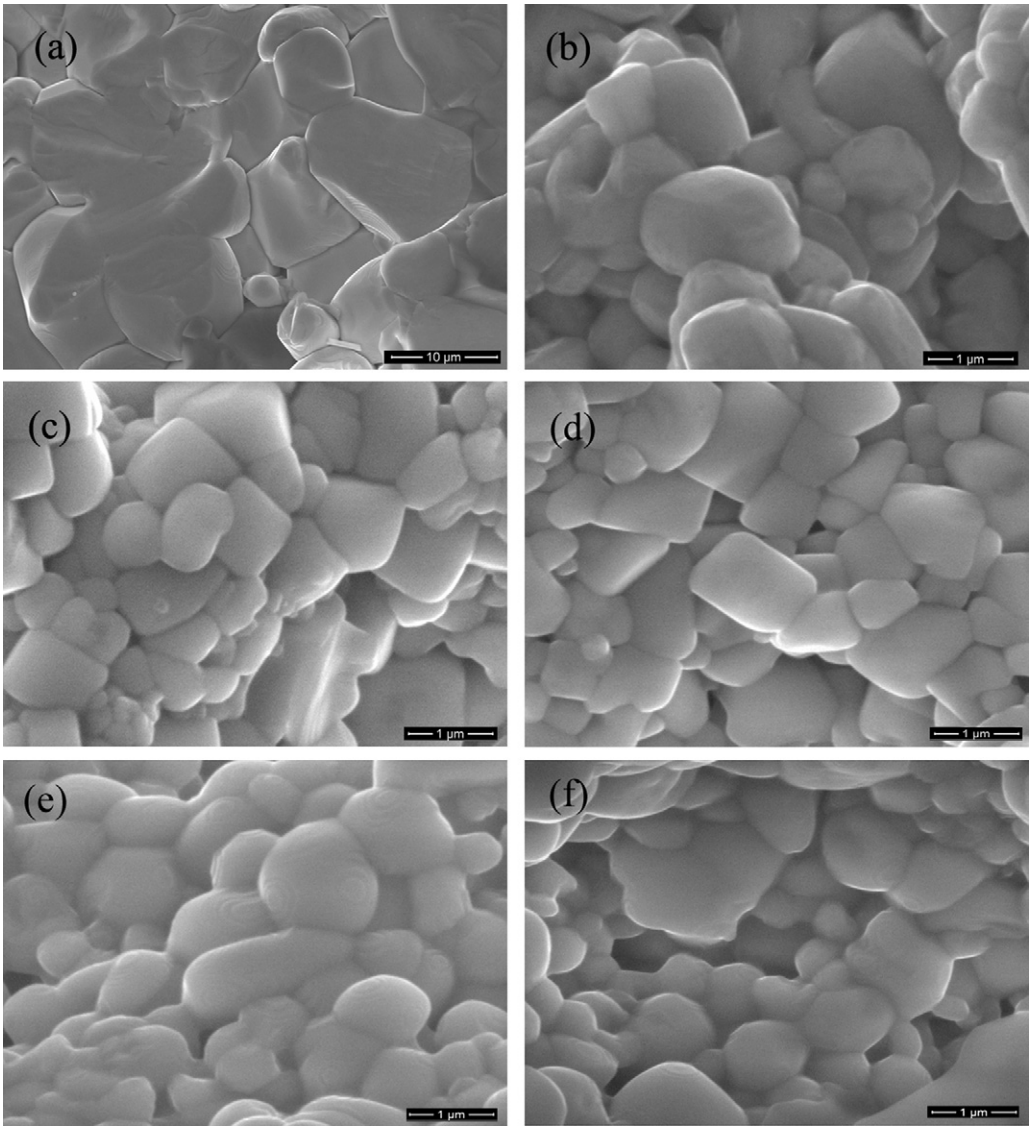

Fig. 2. SEM images of fracture surface of the sintered samples: (a) B6M0, (b) B6M5, (c) B6M15, (d) B6M20, (e) B6M25 and (f) B6M30.

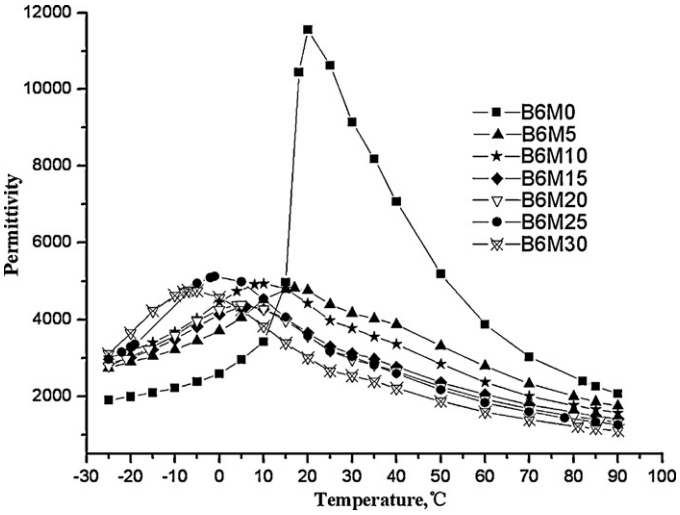

Fig. 3. Temperature dependences of relative dielectric constant for all sintered samples.

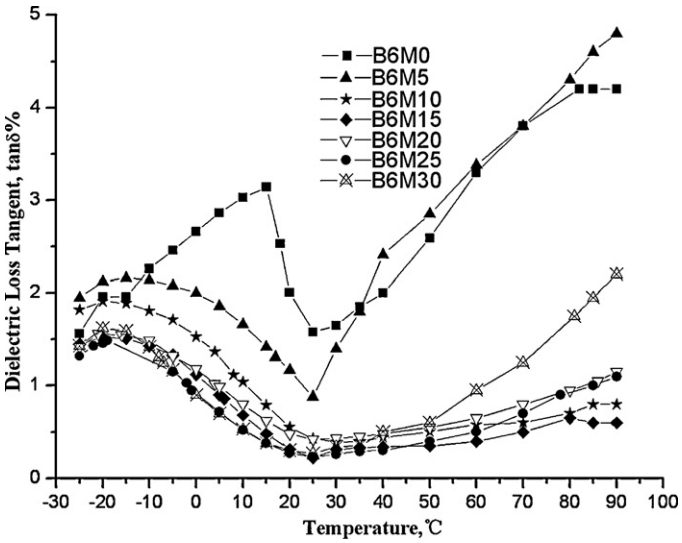

Fig. 4. Temperature dependences of dielectric loss for all sintered samples.

Phase compositions of the samples were analyzed by using X-ray diffractometer (XRD; Model GIRAKU D/MAX 2500V/PC, Japan). Microstructures of the samples were observed with Scanning electron microscope (SEM Philips XL30ESEM).

Capacitance quantity (C) and loss factor (D) were measured by using a capacitance apparatus (Automatic LCR Meter 4225, China) at 1 kHz. Dielectric constant (ε_r) and dielectric loss tangent ($\tan\delta$) were calculated as follows:

$$\varepsilon_r = \frac{14.4Ch}{\phi^2}$$

$$\tan\delta = \frac{fD}{1000}$$

where C and D are the measured capacitance quantities (pF) and loss factors of the samples, respectively. h, φ, and f are thickness (cm), diameter (cm) and frequency, respectively. Temperature dependence of dielectric constant and dielectric loss tangent ($\tan\delta$) were obtained at temperatures ranging from −25 °C to 90 °C. Curie temperature (T_C) was determined from the temperature dependence of dielectric constant.

3. Results and discussion

3.1. Crystal structure and microstructure

Fig. 1 shows XRD patterns of all sintered samples. It can be seen that all samples have a perovskite structure at room temperature. When $x \leq 0.015$, crystalline symmetry of the ceramics is cubic. On the other hand, when $x > 0.015$, the splitting of (2 1 1) peak indicates that there is a distortion in the cubic lattice. Especially, the slight splitting of (2 0 0) peak in Fig. 1(b) indicates that tetragonal and cubic phases coexist in B6M30. In previous works [22,23], Mg^{2+} was reported to act as an acceptor to replace Ti^{4+} of the B site of the perovskite structure, because Mg^{2+} is similar to Ti^{4+} in radius. In this work, the deformation of cubic lattice implies that Mg^{2+} substituted Ti^{4+} of B-site of the perovskite structure and then oxygen vacancies ($V_{O}^{\cdot\cdot}$) formed when $x > 0.015$.

$$MgO(-TiO_2) \Leftrightarrow Mg''_{Ti} + V_O^{\bullet\bullet} + O_0 \quad (1)$$

Fig. 2 shows SEM images of fracture surface of the sintered samples. Grain size of B6M0 is 8–12 μm while grain size of the Mg-doped samples is 0.5–1 μm.

3.2. Dielectric and ferroelectric properties

Fig. 3 shows temperature dependences of relative dielectric constant of all samples. It is obvious that dielectric constant peaks (ε_{max}) of the Mg-doped ceramics are markedly broadened and reduced as compared to B6M0. This behavior is attributed to the small grain sizes of the doped samples. As is well known, a decrease in the grain size causes an increase in fraction of grain boundary, which is non-ferroelectric, and thus leads to the reduction of ε_{max}.

Temperature dependences of dielectric loss of all samples are shown in Fig. 4. Dielectric losses of B6M0 and B6M5 increase greatly at above 25 °C. At $x \geq 0.010$, the addition of Mg^{2+} reduces significantly dielectric losses of the samples over 20–90 °C. It has been widely accepted that A-site vacancies (V_A'') may appear in Bi-doped perovskite-type ceramics to compensate for the charge imbalance arising from the substitution of A-site ions by Bi^{3+} ions [20,21,24]. The presence of vacancies and defects would cause larger losses at higher temperatures. Therefore, dielectric losses of B6M0 and B6M5 above 25 °C are mainly related to A-site vacancies (V_A''). The obvious decrease in dielectric losses for the samples with $x \geq 0.010$ over 20–90 °C implies that Mg^{2+} (0.72 Å) replaced Bi^{3+} (1.38 Å) at A-site of the perovskite structure and thus reduced A-site vacancies (V_A''). At $x \geq 0.010$, most Bi^{3+} was replaced by Mg^{2+} and there were almost no A-site vacancies (V_A''). Most likely, some Bi^{3+} ions were from the lattice by Mg^{2+} and were concentrated at grain boundaries, which caused grain-boundary pinning and thus led to the marked decrease in grain size and thus the decrease in ε_{max}. Dielectric loss of B6M30 increases markedly at above 50 °C, which is related mainly to the high concentration of oxygen vacancies ($V_{O}^{\cdot\cdot}$) caused by the substitution of Mg^{2+} for Ti^{4+} (Eq. (1)).

In the vicinity of transition temperature, dielectric constant ε_r and Curie temperature T_C corresponding to dielectric constant peaks (ε_{max}) of ferroelectric crystals can be described by the Curie–Weiss law:

$$\varepsilon_r = \frac{C}{T - T_0} \quad (2)$$

where C is Curie constant and T_0 is Curie–Weiss temperature, respectively. Fig. 5 shows plots of inverse dielectric constant versus temperature for all samples. Ferroelectric–paraelectric phase transition is of first order at $T_0 < T_C$ and of second order at $T_0 = T_C$. It can be seen that inverse dielectric constant versus temperature of B6M0 and B6M30 deviates from Curie–Weiss law above phase transition temperature, which reveals a diffuse phase transition [25]. This phenomenon may be ascribed to disordering caused by compositional fluctuation and structural defects [26,27]. In addition, Zhou et al. [21] proposed that, Bi^{3+} ions substituting for Sr^{2+} in perovskite structure ABO_3 can be located at off-center positions, and then a random electric field formed by off-center Bi^{3+}

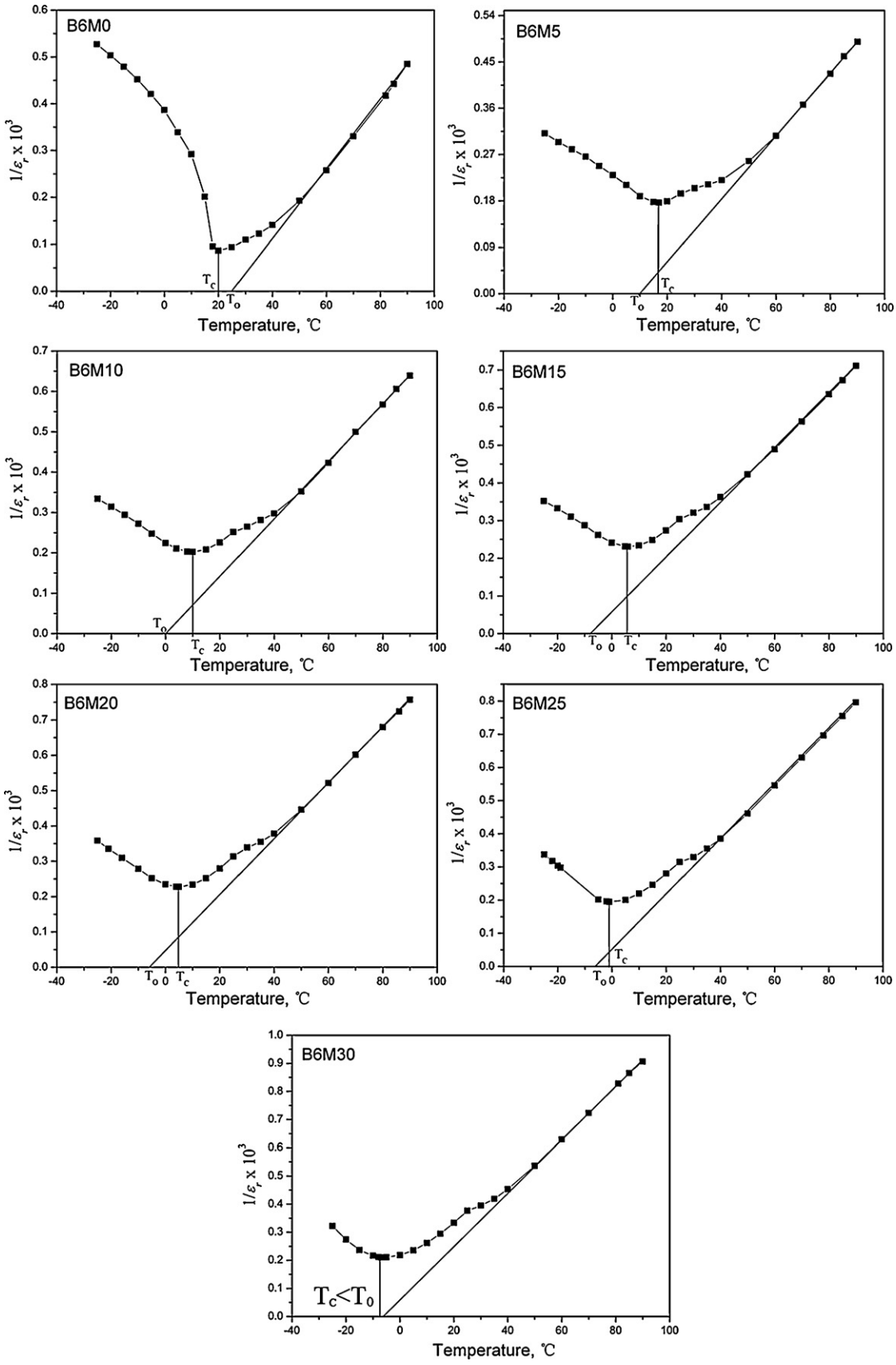

Fig. 5. Temperature dependences of $1/\varepsilon_r$ for all sintered ceramics.

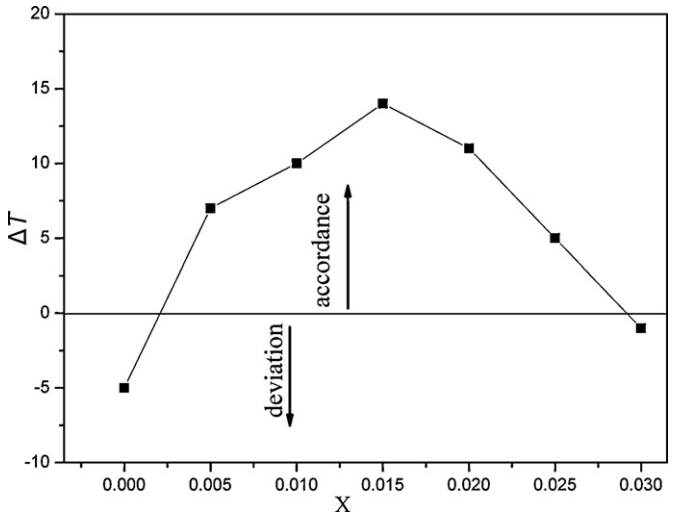

Fig. 6. ΔT of the ceramics as a function of Mg^{2+} content.

ions and Bi^{3+}–V_A'' dipoles would increase diffuseness. For B6M0, the diffuse phase transition may be associated with V_A'' (structural defects) and the random electric field. According to above analysis, the off-center Bi^{3+} ions and Bi^{3+}–V_A'' dipoles were almost nonexistent in B6M30, but there were Mg_{Ti}'' and $V_O^{\cdot\cdot}$, accordingly a random electric field were also formed by Mg_{Ti}''–$V_O^{\cdot\cdot}$. Therefore, random electric field and as well as $V_O^{\cdot\cdot}$ (structural defects) resulted in the diffuse phase transition of B6M30. The samples with compositions of $0.005 \le x \le 0.025$ abide the conventional Curie–Weiss law above phase transition temperature. The phase transitions are of first order. In order to describe the degree of obedience to the Curie–Weiss law, ΔT is defined as

$$\Delta T = T_C - T_0 \quad (3)$$

The plot of ΔT versus x (Mg^{2+} content) is shown in Fig. 6. Obviously, ΔT increases with the increase of Mg^{2+} content at $x \le 0.015$, but it decreases with increasing Mg^{2+} at $x > 0.015$. This again implies that Mg^{2+} replaced Bi^{3+} at A-site in the perovskite structure and the concentration of A-site vacancies (V_A'') and the random electric field decreased at $x \le 0.015$, but at $x > 0.015$, Mg^{2+} substituted Ti^{4+} at B-site of the perovskite structure and thus there were more structural defects ($V_O^{\cdot\cdot}$) and the random electric field.

From the above, Mg^{2+} would counteract effect of Bi^{3+} on the diffuse phase transition of $(Ba_{0.68}Sr_{0.311}Bi_{0.006})(Ti_{0.99}Sn_{0.01})O_3$.

3.3. Electric conduction

Fig. 7 shows temperature dependences of conductance of the samples at DC, 10 kHz AC, 1 kHz AC, and 100 Hz AC. According to Arrehenius relationship (Eq. (4)), we fitted the curves to obtain E_a

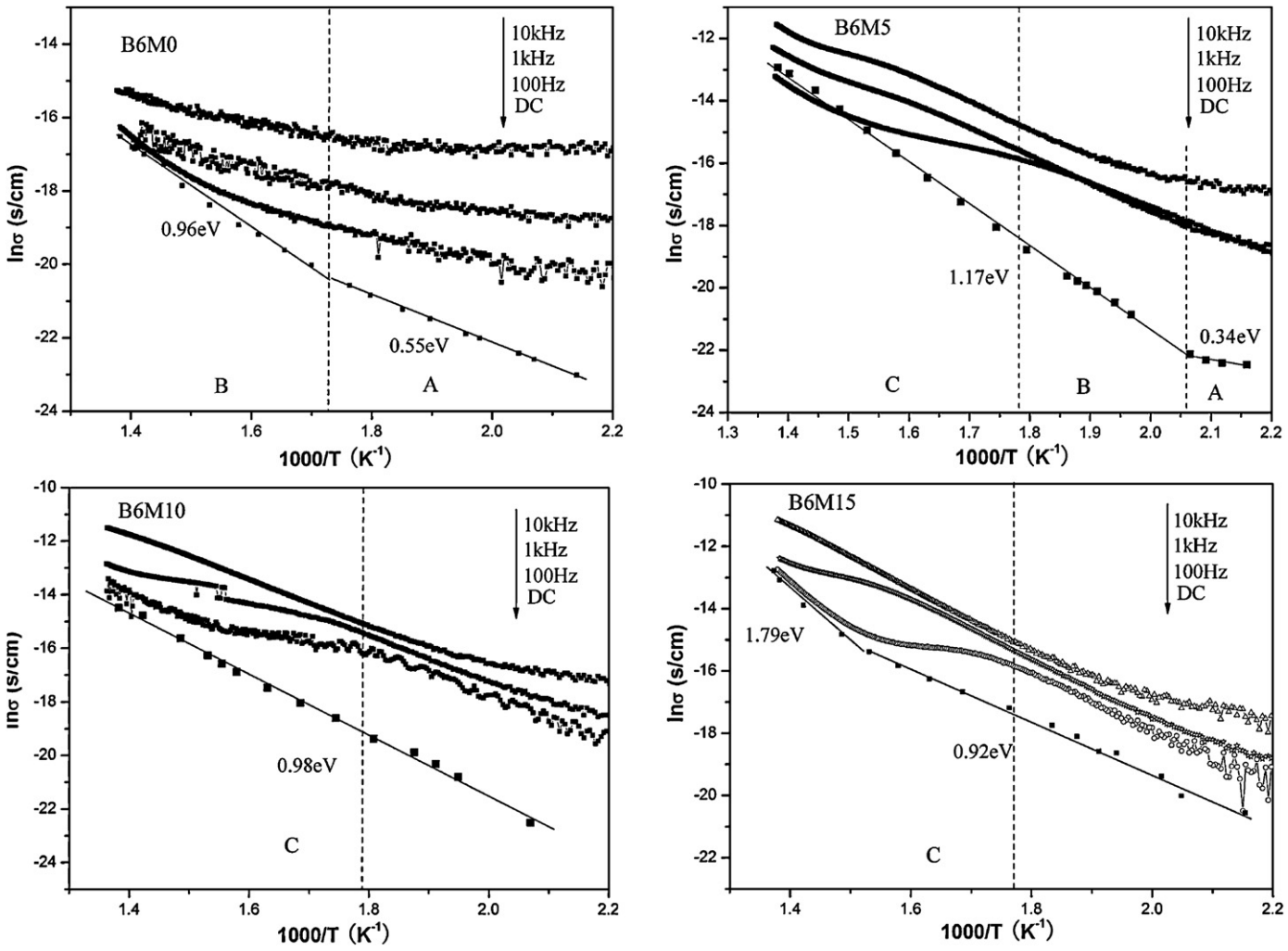

Fig. 7. DC and AC conductivities of all ceramics.

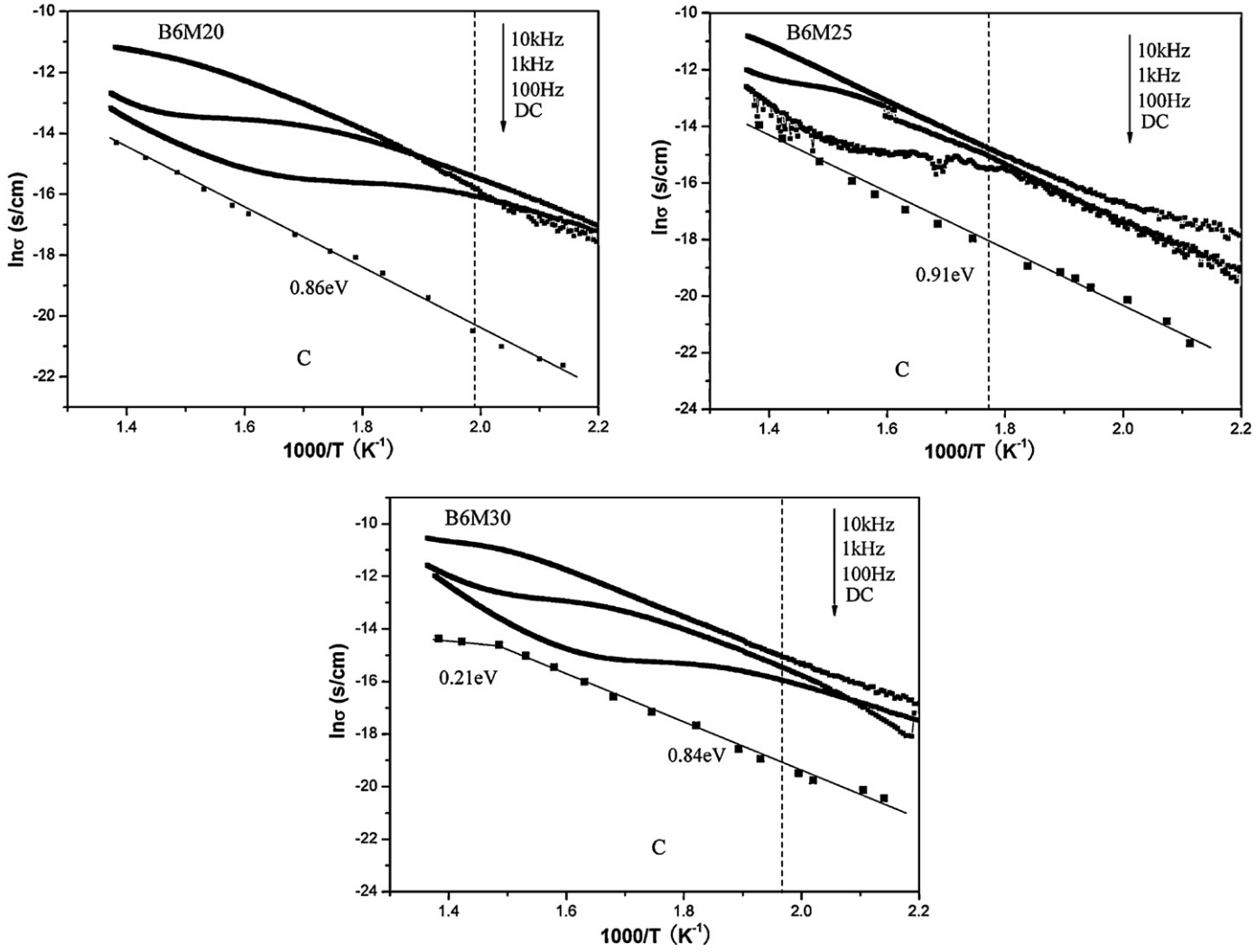

Fig. 7. *(Continued)*

at DC (200–450 °C) for all samples.

$$\sigma = \sigma_0 \exp\left(\frac{-E_a}{kT}\right) \quad (4)$$

where σ_0 is a pre-exponential factor, E_a is the activation energy and k is the Boltzmann constant. The samples B6M0 and B6M5 have strong frequency dependence and small E_a at DC (0.55 eV and 0.34 eV) in region A. This observation may be related to vacancy transition (V_A'') and hole ($h^\bullet$) for charge compensation of V_A''. On the other hand, all ceramics, except B6M0, demonstrate E_a of 0.84–1.17 eV and frequency dispersions in the region Wei et al. [28] attributed this frequency dispersion to hopping of localized hole ($h^\bullet$), which was formed via oxidation of oxygen vacancies.

$$\frac{1}{2}O_2 + V_O^{\bullet\bullet} \Leftrightarrow O_0 + 2h^\bullet \quad (5)$$

In region B, for B6M0, E_a of 0.96 eV is close to those of other samples. Therefore, it can be concluded that the conduction carriers are also the holes ($h^\cdot$) controlled by $V_O^{\cdot\cdot}$, which were caused by volatilization of Bi^{3+}. But only when temperature is above 300 °C, E_a of B6M0 is close to those of other samples. This may be related to more V_A'' which can trap the holes ($h^\cdot$).

4. Conclusions

Structure, dielectric and electric properties of $(Ba_{0.68-x}Sr_{0.311}Bi_{0.006}Mg_x)(Ti_{0.99}Sn_{0.01})O_3$ ceramics were influenced by the content of Mg^{2+}. At lower Mg^{2+} concentrations ($x \leq 0.015$), Mg^{2+} replaced Bi^{3+} at A-site in the perovskite structure, which made dielectric constant of the samples to obey the Curie–Weiss law above phase transition temperature. The Bi^{3+} ions were expelled from the lattice by Mg^{2+} and concentrated at grain boundaries, which caused a significant decrease in grain size and thus ε_{max}. At higher Mg^{2+} concentrations ($x > 0.015$), Mg^{2+} acted as an acceptor to replace Ti^{4+} at B-site of the perovskite structure, leading to a deformation of the cubic lattice and thus making dielectric constant of the samples to deviate from the Curie–Weiss law above phase transition temperature. In high temperature region, the conduction carriers of all samples were controlled by $V_O^{\cdot\cdot}$.

Acknowledgement

This research was supported by the Chinese Doctor Foundation of National Ministry of Education (Grant no. 20040056055).

References

[1] A. Ioachim, M.I. Toacsan, M.G. Banciu, L. Nedelcu, F. Vasiliu, H.V. Alexandru, C. Berbecaru, G. Stoica, Prog. Solid State Chem. 35 (2007) 513.
[2] Y. Ota, K.I. Kakimoto, H. Ohsato, T. Okawa, J. Eur. Ceram. Soc. 24 (2004) 1755.
[3] Y.C. Chen, P.S. Cheng, C.F. Yang, W.C. Tzou, Ceram. Int. 27 (2001) 809.
[4] H. Zhou, H. Wang, Y. Chen, K. Li, X. Yao, Mater. Chem. Phys. 113 (2009) 1.
[5] R. Zuo, X. Fang, C. Ye, Appl. Phys. Lett. 90 (2007) 092904.
[6] J. Qi, Z. Gui, W. Li, Y. Wang, Y. Wu, L. Li, Mater. Lett. 56 (2002) 507.
[7] L.P. Curecheriu, L. Mitoseriu, A. Ianculescu, J. Alloys Compd. 482 (2009) 1.
[8] A.K. Nath, K.C. Singh, R. Laishram, O.P. Thakur, Mater. Sci. Eng. B 172 (2010) 151.
[9] G. Aldica, M. Cernea, R. Radu, R. Trusca, J. Alloys Compd. 505 (2010) 273.
[10] V.V. Shvartsman, W. Kleemann, J. Dec, J. Appl. Phys. 99 (2006) 124111.
[11] S. Lu, Z. Xu, Appl. Phys. Lett. 92 (2008) 232907.
[12] I.A. Souza, L.S. Cavalcante, J.C. Sczancoski, F. Moura, C.O. Paiva-Santos, J.A. Varela, A.Z. Simões, E. Longo, J. Alloys Compd. 477 (2009) 877.
[13] G. Aldica, M. Cernea, P. Ganea, J. Mater. Sci. 45 (2010) 2606.
[14] S. Suzuki, T. Takeda, A. Ando, H. Takagi, Appl. Phys. Lett. 96 (2010) 132903.
[15] S.G. Lu, Z.K. Xu, H. Chen, Appl. Phys. Lett. 85 (2004) 5319.
[16] W. Chen, X. Yao, X. Wei, Appl. Phys. Lett. 90 (2007) 182902.
[17] S. Marković, M. Mitrić, N. Cvjetićanin, D. Uskoković, J. Eur. Ceram. Soc. 27 (2007) 505.
[18] F. Du, B. Cui, H. Cheng, R. Niu, Z. Chang, Mater. Res. Bull. 44 (2009) 1930.
[19] Y. Liu, R.L. Withers, X. Wei, J.D.F. Gerald, J. Solid State Chem. 180 (2007) 858.
[20] T. Badapanda, S.K. Rout, S. Panigrahi, T.P. Sinha, Curr. Appl. Phys. 9 (2009) 727.
[21] L. Zhou, P.M. Vilarinho, J.L. Baptista, J. Eur. Ceram. Soc. 21 (2001) 531.
[22] S. Xu, Y. Qu, C. Zhang, J. Appl. Phys. 106 (2009) 014107.
[23] B. Su, T.W. Button, J. Appl. Phys. 95 (2004) 1382.
[24] S. Yun, X. Wang, J. Li, J. Shi, D. Xu, Mater. Chem. Phys. 116 (2009) 339.
[25] S.K. Rout, E. Sinha, S. Panigrahi, Mater. Chem. Phys. 101 (2007) 428.
[26] C.G.F. Stenger, A.I. Buggraaf, J. Phys. Chem. Solids 41 (1980) 25.
[27] L.E. Cross, Ferroelectrics 76 (1987) 241.
[28] X. Wei, X. Wan, X. Yao, J. Electroceram. 21 (2008) 226.